

# Photo-Thermo-Mechanical Model for Laser Hair Removal Simulation using Multiphysics Coupling of Light Transport, Heat Transfer, and Mechanical Deformation (Case Study)

Vannakorn Mongkol, Wutipong Preechaphonkul, and Phadungsak Rattanadecho\*

Center of Excellence in Electromagnetic Energy Utilization in Engineering (CEEE), Department of Mechanical Engineering, Faculty of Engineering, Thammasat University, Khlong Luang, Pathum Thani, Thailand 12120

\* Corresponding author E-mail address: [ratphadu@engr.tu.ac.th](mailto:ratphadu@engr.tu.ac.th)

## Abstract

The mathematical model has become one of the tools for prediction to assist physicians and specialists with hair laser removal in dermatology. This paper proposes a model that comprehensively predicts optical, thermal, and mechanical responses within the skin during laser hair removal to determine optimal therapeutic conditions and prevent skin tissue damage. This research highlighted developing a mathematical model using multiple physics of light transport, heat transfer, and mechanical deformation. The present mathematical model is resolved using the 2D axisymmetric finite element method (FEM) with optical, thermal, and mechanical properties to characterize the laser intensity, temperature distribution, mechanical stress, and displacements within skin tissue. The comparison of the simulated results in laser wavelengths of 595 nm, 800 nm, and 1064 nm is also provided. The results revealed that laser deposition with skin tissue depends on the wavelength and optical diffusion coefficient. Applying the 1064 nm performs the best treatment outcome for hair laser removal. In contrast, 595 nm and 800 nm might lead to adverse pain sensations. The high temperature caused an increase in mechanical stress and displacement. The results of this study indicate that laser therapy has certain limitations that must be considered.

**Keyword** : Laser hair removal, Light transport, Bioheat, Mechanical Deformation, Photo-Thermo-Mechanical model, Numerical simulation.

## 1. Introduction

Recently, laser has caught the attention of researchers, utilizing it in medical treatments such as dermatology [1]. Laser hair removal is one of the medical applications. It is a medical process that employs intense light and pulses to permanently eliminate hair from the armpits, legs, shins, face, and even private parts [2]. Hair follicles have a high melanin content filled with stem cells capable of repairing the hair follicle, and hair is the primary target tissue. The hair follicle can be destroyed and entirely removed at a temperature of 65 °C. [3-4]. The destruction of hair follicles depends on several factors, such as suitable wavelength, pulse size, and intensity [5]. When skin and targeted tissue receive laser irradiation, the energy from the laser will be absorbed and produce heat within the tissue. Healthy tissue in the surrounding area may experience undesired heating, leading to thermal damage and pain during laser hair removal. The research found that negative sensations and emotional experiences cause pain [6]. Human skin tissues respond to thermal, mechanical, and chemical stimuli with thermal and mechanical sensitivity of 43 °C and 0.2 MPa, respectively.[7] Hence, it is necessary to govern and decrease heat transfer inside the targeted tissue, leading to damage prevention of surrounding tissues. Physicians and researchers have been studying physiological phenomena inside human skin for tissue damage prevention while removing hair with laser therapy, producing and developing more efficient and safer equipment. [8]

Several researchers have studied laser treatments for hair removal, e.g., Goldberg et al. [10] investigated the efficacy of hair removal on various body parts using a laser at different intensities and discovered that the size of the laser intensity affects the regeneration of hair. There are other experimental studies also included animal testing [11-15] In recent years have seen an increase in the use of mathematical models due to their benefits, which include cost savings, shorter study times, the ability to define a broad range of treatment conditions, Etc. Researchers have presented mathematical models for laser hair removal. In 2009, Sun et al.[15] proposed a Fourier model to predict temperature profiles of human skin for laser hair removal, which considers optical properties of melanin, water, and blood in the human skin. It was discovered that the average temperature of hair follicles rises as a linear function of fluence. Additionally, there are studies of thermal damage investigation for unwanted heat prevention using mathematical models for laser hair removal, which indicate that applying a small spot size and fluence, including using a long pulse duration, can reduce thermal damage area. [16-17]. In 2014, Kim and Lee proposed a mathematical model that studied the effect of color skin types on temperature profiles for laser hair

1 removal and found that dark skin can lead to more adverse effects [18]. In 2019, a 3D human skin model was proposed by  
2 Mármol and Villena [19] to evaluate the safety and efficacy of laser wavelengths and cooling devices for laser hair removal  
3 treatment and thermal injury prevention. In addition, there are many related studies [20-27] on the development of  
4 mathematical models using laser therapy, such as the study of phase change effect on temperature [24], tumor ablation  
5 [20,21], and increasing the efficiency of light absorption through nanoparticle injection [26,27], as well as the cooling effect  
6 of blood circulation in blood vessel embedded in the skin [22,23]. Most simulation studies of laser treatment in dermatology  
7 and previously mentioned works widely used the non-Fourier model of Pennes's bioheat equation in the mathematical model,  
8 induced by Pennes [28], for solving heat problems in bio-material [16-27,29-36].

9 In addition, when skin tissue is exposed to high temperatures during thermotherapy induced by laser, mechanical  
10 stress occurs within the skin tissue due to thermal denaturation, resulting in the deformation of the skin [37]. Moreover,  
11 thermal and mechanical energy converts to ionic current, resulting in the sensation of physical pain during therapeutic [38].  
12 Few researchers have presented models to investigate mechanical response of human skin due to thermal effects. Jor et al.  
13 [39] developed a 3D discrete fiber skin model and discovered that the deformation was related to density, fiber thickness,  
14 and tissue stiffness. Garaizar et al.[40] developed a model to investigate the mechanical effects of the skin from the thermal  
15 and external load. Moreover, Larrabee [41] proposed a model to study the human skin's mechanical and viscoelastic  
16 properties. The viscoelastic properties permit better movement of skin structures without rupturing compared to elastic  
17 properties, which protect against injury of skin tissue. Recently, In previously published work, Wongchadaku et al.[25]  
18 presented the 2D asymmetric model of human skin to study the influence of wavelength, intensities, and irradiation time on  
19 the human skin's mechanical response during laser treatment. Furthermore, some studies study the mechanical stain from  
20 thermal effects in biological tissues as well, such as breast and liver cancer [34,42].

21 From literature exploration, we observed that in the past research on mathematical modeling of laser hair removal  
22 and other laser therapy, Beer-Lambert's law is used to calculate laser deposition within skin tissue since it is simple to apply  
23 and avoids increasing the complexity of the mathematical model [16-18,21,25-27]. Nevertheless, the optical diffusion  
24 coefficient, one of the essential parameters of light diffusion in the medium that must be calculated systematically, is required.  
25 For a comprehensive analysis, laser energy deposition within dermal tissue has to be analyzed using the light transport  
26 equation, which has been used in previous studies[14,19,43-45]. In another observation, previous research concentrated on  
27 modeling for studying thermal behavior from the effects of wavelengths, beam diameters, and laser intensities. In contrast,  
28 investigating the mechanical phenomenon of the skin of laser hair removal remains challenging as evidence has shown that  
29 there are few studies have examined the mechanical effects, e.g., thermal stress and skin displacement, another critical factor  
30 that might directly affect pain sensation during laser hair removal and other therapy. Further, we observed that there are a  
31 few research that proposes a mathematical model using Multiphysics of the light transport equation, heat transfer, and  
32 mechanical deformation for laser hair removal.

33 Therefore, this present study employs a photo-thermo-mechanical model to predict the thermal and mechanical  
34 response of laser hair removal. The current model is one of the few mathematical modelings of laser hair removal using  
35 multiple physics of light transport, bioheat transfer, and mechanical deformation and is developed based on a 2D  
36 axisymmetric model. The model utilized the laser deposition energy described by the light transport equation instead of Beer-  
37 Lambert's law, and Pennes's bioheat equation describes the transient temperature of skin tissue. In addition, the equilibrium  
38 equation is used to analyze the mechanical deformation within tissue. Within the context of this model, numerical research  
39 was conducted to investigate the impact that wavelengths have on the laser intensity, temperature distribution, Von-Mises  
40 stress, and total displacement in the skin. Therefore in the study, the numerical simulation results mentioned above were  
41 compared. The findings of this study can be used to enhance the phenomena that must be considered for adequate therapy  
42 preparation and therapeutic outcomes and to be a sample for further development in other related mathematical modeling  
43 work.

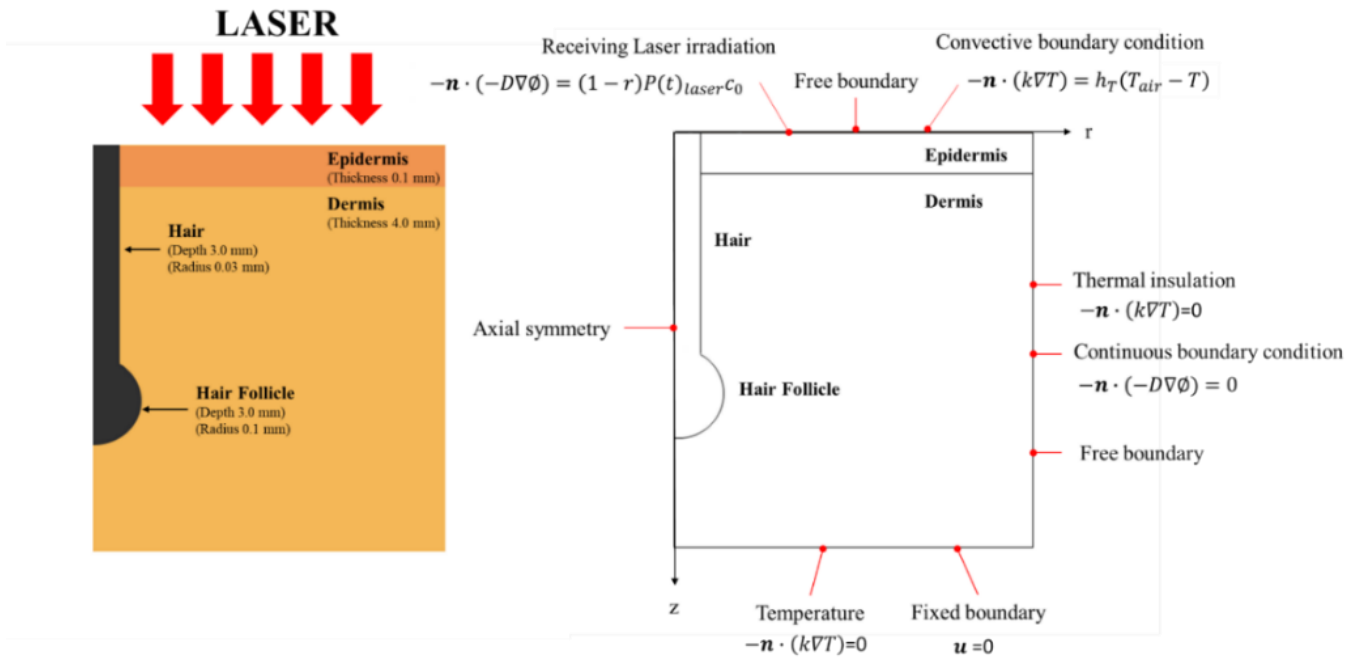
## 44 **2. Problem description**

45  
46  
47 Laser hair removal is the chosen method for physicians and aesthetic specialists for hair removal on various parts of  
48 the human body. The outer layer of the skin is irradiated with a laser to heat it to its hair-eliminating temperature. The negative  
49 aspect of using laser techniques for hair removal is the undesired heat to surrounding tissue, which may cause thermal injury  
50 to healthy tissue and pain during therapy. However, there are two primary pain sensations: thermal and mechanical. The high  
51 temperature and mechanical stress within skin tissue might also have adverse effects. A comprehensive investigation of  
52 thermal and mechanical phenomena is still challenging for appropriate therapeutic preparation. Consequently, we presented  
53 the photo-thermo-mechanical model. The proposed model was utilized to examine the temperature distribution, Von-Mises  
54 stress, and total skin displacement during laser hair removal.

1  
2  
3  
4  
5  
6  
7  
8  
9  
10  
11  
12  
13  
14  
15

### 3. Method and Model

The focus of the study was on the thermal and mechanical responses of skin and hair during laser hair removal. Laser energy calculation is the first step in understanding laser deposition within skin tissue. Then, the light energy absorbed, which led to an increase in temperature and was related to mechanical deformation phenomena in skin tissue, was examined. For the modeling, the model is created under a two-dimensional (2D) axisymmetric in a cylindrical coordinate system for mathematical modeling. The mathematical model considers the light transport, heat transfer, and mechanical deformation in skin tissue using the COMSOL Multiphysics software based on the Finite Element Method (FEM). The light transport equation, Pennes's bioheat equation, and the equilibrium equation are used to calculate the deposition of laser light, heat transfer, and mechanical deformation within skin tissue. Pennes's bioheat equation analyzes the heat diffusion within the skin tissue. We used wavelengths of 595 nm, 800 nm, and 1064 nm for providing the temperature, Von Mises stress, and skin displacement. The model properties were referred to in the literature [12-15,18,25,46-56] and shown in Table 1.



16  
17  
18  
19  
20  
21  
22  
23  
24  
25  
26  
27  
28  
29  
30  
31  
32  
33  
34  
35  
36

Figure 1. Physical domain and boundary conditions.

#### 3.1 Physical model for numerical analysis

According to the biological structure of human skin, skin tissue contains several organs. In this study, the structure of the skin has been simplified. The photo-thermo-mechanical model consists of multilayers of the epidermis, dermis, hair, and hair follicles. Figure.1 shows a 2D axisymmetric skin model and details obtained from the literature. [14,49-50]. Moreover, this model considers the effect of light reflection on the skin surface. The light transport equation describes the laser deposition with skin tissue as the effect of light absorption and scattering. All properties are taken directly from the literature.[12-15,18,25,46-56]

For problem simplification, the following assumptions have been made:

1. The model is considered in the two dimensions of axisymmetric analysis.
2. The material properties of skin tissues are assumed to be isotropic and homogeneous.
3. The interfaces between tissues are considered to be smooth interfaces.
4. Phase change and chemical reactions within skin tissues are ignored.

#### 3.2 Equation for light transport analysis

Light transport is considered in all domains and is described by the following differential equation [44] :

$$\frac{\partial}{\partial t} \phi - D \nabla^2 \phi + c_{e,d,h} \mu_a \phi = 0 \quad (1)$$

$$D = c_{e,d,h} [3(\mu_a + (1 - g)\mu_s)]^{-1} \quad (2)$$

Where  $\phi$  is the intensities of laser ( $\text{W}/\text{m}^2$ ),  $D$  is the optical diffusion coefficient ( $\text{m}^2/\text{s}$ ) of skin tissue,  $c_{e,d,h}$  is the speed of light in the epidermis, dermis or hair,  $\mu_a$  is the absorption coefficient ( $1/\text{m}$ ) of skin,  $\mu_s$  is the scattering coefficient ( $1/\text{m}$ ) and  $g$  is the optical anisotropy factor.

### 3.2.1 Boundary conditions for light transport analysis

On the skin surface, it assumed that laser continually and uniformly exposure irradiation along the boundary conditions [44] as shown in the Figure.1

$$-\mathbf{n} \cdot (-D \nabla \phi) = (1 - R) P(t)_{laser} c_0 \quad (3)$$

Where  $P(t)_{laser}$  is the laser irradiance at the upper surface ( $\text{W}/\text{m}^2$ ),  $c_0$  is speed of light in vacuum and  $R$  is the ratio of reflected light.

The lower and outer surface were assumed that laser flux continuous boundary condition.

$$-\mathbf{n} \cdot (-D \nabla \phi) = 0 \quad (4)$$

### 3.3 Equations for heat transfer analysis

Pennes's bioheat is considered in all domains to analyze heat transfer within each tissue. [28]

$$\rho C \frac{\partial T}{\partial t} = \nabla \cdot (k \nabla T) + \rho_b C_b \omega_b (T_b - T) + Q_{met} + \mu_a \phi \quad (5)$$

Where  $\rho$  is tissue density ( $\text{kg}/\text{m}^3$ ),  $C$  is tissue heat capacity ( $\text{J}/\text{kg} \cdot \text{K}$ ),  $k$  is tissue heat conductivity ( $\text{W}/\text{m} \cdot \text{K}$ ),  $T$  is tissue temperature ( $^{\circ}\text{C}$ ),  $\rho_b C_b \omega_b (T_b - T)$  is the blood perfusion term,  $T_b$  is the blood temperature ( $36^{\circ}\text{C}$ ) [25],  $\rho_b$  is the blood density ( $1,060 \text{ kg}/\text{m}^3$ ) [25],  $C_b$  is the specific heat capacity of the blood ( $3,660 \text{ J}/\text{kg} \cdot \text{K}$ ) [25],  $\omega_b$  is the rate of blood perfusion ( $1/\text{s}$ ),  $Q_{met}$  is Metabolic heat generation ( $\text{W}/\text{m}^3$ ), and considering of term external heat sources of laser deposition ( $\text{W}/\text{m}^3$ ).

#### 3.3.1 boundary condition for heat transfer analysis

The boundary conditions are specified in Figure.1 and the skin surface is under convection boundary conditions:

$$-\mathbf{n} \cdot (k \nabla T) = h_T (T_{air} - T) \quad (6)$$

Where  $T_{air}$  is the ambient temperature ( $20^{\circ}\text{C}$ ) and  $h_T$  is heat transfer coefficient ( $10 \text{ W}/(\text{m}^2 \cdot \text{K})$ )

The internal interfaces between each tissue are a smooth condition which means no contact thermal resistance. So, it is assumed to be under a continuity boundary condition.

$$\mathbf{n} \cdot (k_u \nabla T_u - k_d \nabla T_d) = 0 \quad (7)$$

#### 3.4 Equation for mechanical deformation analysis

As presented in previous studies [25,41,42], the model is simplified to a quasi-static model. The mechanical deformation such as displacements and stresses occurring within skin tissue that exposure laser light was investigated by using the equilibrium equations (equation (8a-8b)), the stress-strain relationship (equation (9a)-(9c)), and the strain-displacement relationship (equation (10a)-(10b)) described in cylindrical coordinate systems [42].

$$\frac{\partial \sigma_{rr}}{\partial r} + \frac{\partial \sigma_{rz}}{\partial z} + \frac{\sigma_{rz} - \sigma_{\theta\theta}}{r} + F_r = \rho \frac{\partial^2 u_r}{\partial t^2} \quad (8a)$$

$$\frac{\partial \sigma_{rz}}{\partial r} + \frac{\partial \sigma_{zz}}{\partial z} + \frac{\sigma_{rz}}{r} + F_z = \rho \frac{\partial^2 u_z}{\partial t^2} \quad (8b)$$

$$\epsilon_{rr} = \frac{1}{E} [\sigma_{rr} - \nu(\sigma_{\phi\phi} + \sigma_{zz})] + \epsilon^{th} \quad (9a)$$

$$\epsilon_{zz} = \frac{1}{E} [\sigma_{zz} - \nu(\sigma_{\phi\phi} + \sigma_{rr})] + \epsilon^{th} \quad (9b)$$

$$\epsilon_{\phi\phi} = \frac{1}{E} [\sigma_{\phi\phi} - \nu(\sigma_{rr} + \sigma_{zz})] + \epsilon^{th} \quad (9c)$$

$$\epsilon_{rr} = \frac{\partial u_r}{\partial r}, \epsilon_{zz} = \frac{\partial u_z}{\partial z}, \epsilon_{\phi\phi} = \frac{u}{r}, \quad (10a)$$

$$\epsilon_{rz} = \frac{1}{2} \left( \frac{\partial u_r}{\partial z} + \frac{\partial u_z}{\partial r} \right) \quad (10b)$$

$$\epsilon^{th} = \int_{T_{ref}}^T \alpha dT \quad (11)$$

Where  $\sigma$  is the stress (Pa),  $\epsilon$  is the strain,  $F$  is the external volumetric force ( $0 \text{ N/m}^3$  for here),  $E$  is Young's modulus (Pa),  $\nu$  is the Poisson's ratio and  $u$  is the displacement (m).  $\epsilon^{th}$  is the thermal strain,  $\alpha$  is the coefficient of thermal expansion ( $1/^\circ\text{C}$ ) and  $T_{ref}$  is  $36 \text{ }^\circ\text{C}$  the reference temperature.

### 3.4.1 Boundary condition for mechanical deformation analysis

The bottom surface is fixed constraint boundary condition. The rest of boundary is considered free boundary condition and the initial stress and strain are set to zero:

$$\sigma_{ri}, \sigma_{\phi i}, \sigma_{zi} \text{ and } \sigma_{rzi} = 0 \text{ Pa} \quad (12)$$

$$\epsilon_{ri}, \epsilon_{\phi i}, \epsilon_{zi} \text{ and } \epsilon_{rzi} = 0 \quad (13)$$

### 3.5 Initial conditions

The initial value of light deposition is  $0 \text{ W/m}^2$ , the initial temperature is  $36 \text{ }^\circ\text{C}$  (core body temperature), and initial displacement field is  $0 \text{ mm}$ .

### 3.6 Calculation procedure

To investigate the phenomenon within the tissue model during the hair laser removal process. FEM is used for solving numerical problems via COMSOL™ Multiphysics. The system of governing equations, boundary conditions, and initial values are systematically calculated. The light transport equation, Pennes's bioheat, and equilibrium equation were applied in all domains. The initial and boundary conditions were followed in the previous section. The discretization of numerical models using triangular, edge, and vertex elements. In independent solving setting, initial and maximum time steps for solving of the transient problem were  $1 \times 10^{-3}$ , s and  $0.1$  s, respectively. The laser intensity within each tissue is obtained by calculating the light transport equation from laser irradiation and then used as input values in the bioheat equation to compute the heat source of laser deposition in each tissue, which raises the tissue temperature later. Simultaneously, the thermal strain was recalculated using the temperature distribution within skin tissue. Until  $50 \text{ ms}$  of irradiation, the laser's intensity, temperature, Von-Mises stress, and displacement are collected. In addition, the optimal number of elements that do not affect results changing for simulation is determined by a convergence test—testing with a wavelength of  $1064 \text{ nm}$ , power of laser  $5 \text{ J/cm}^2$  at laser irradiation  $50 \text{ ms}$ , and properties taken from Table 1. As depicted in Figure.2(d), the results of this convergence test revealed a grid of approximately  $20,000$  elements.

Table.1 Thermal, mechanical and optical properties using in this study [12-15,18,25,46-56]

	Epidermis	Dermis	Hair
Tissue density, $\rho$ (kg/m <sup>3</sup> )	1200	1090	1030
Specific heat of tissue, $C$ (J/(Kg K))	3950	3350	3582
Thermal conductivity, $k$ (W/(m K))	0.24	0.42	0.558
Blood perfusion, $\omega_b$ (1/s)	-	0.0031	-
Metabolic heat generation, $Q_{met}$ (W/m <sup>3</sup> )	368	368	368
Thermal expansion coefficient, $\alpha$ (1/K)	0.0001	0.0001	0.0001
Poisson's ratio (-)	0.48	0.48	0.48
Young's modulus (GPa)	0.102	0.0102	4.1
Absorption coefficient, $\mu_a$ (1/m), 595 nm	1708.49	85.42	6000
Absorption coefficient, $\mu_a$ (1/m), 800 nm	858	24	3800
Absorption coefficient, $\mu_a$ (1/m), 1064 nm	226.03	11.30	2500
Scattering coefficient, $\mu_s$ (1/m), 595 nm	24243.70	24243.70	3844.86
Scattering coefficient, $\mu_s$ (1/m), 800 nm	18031.25	18031.25	1421.08
Scattering coefficient, $\mu_s$ (1/m), 1064 nm	13557.33	13557.33	544.79
Anisotropy, $g$ , 595 nm	0.9	0.79	0.9
Anisotropy, $g$ , 800 nm	0.85	0.85	0.9
Anisotropy, $g$ , 1064 nm	0.85	0.85	0.9
Refractive index, $n$	1.37	1.37	1.37
Ratio of reflected light, 595 nm	0.45	-	-
Ratio of reflected light, 800 nm	0.6	-	-
Ratio of reflected light, 1064 nm	0.5	-	-

1  
2 Table 2. Properties of tissue phantom [23].

Properties	Phantom Tissue (agar)
Tissue density, $\rho$ (kg/m <sup>3</sup> )	1050
Specific heat of tissue, $C$ (J/(Kg K))	4219
Thermal conductivity, $k$ (W/(m K))	0.66
Absorption coefficient, $\mu_a$ (1/m)	530
Scattering coefficient, $\mu_s$ (1/m)	40

3  
4 4. Validation of model

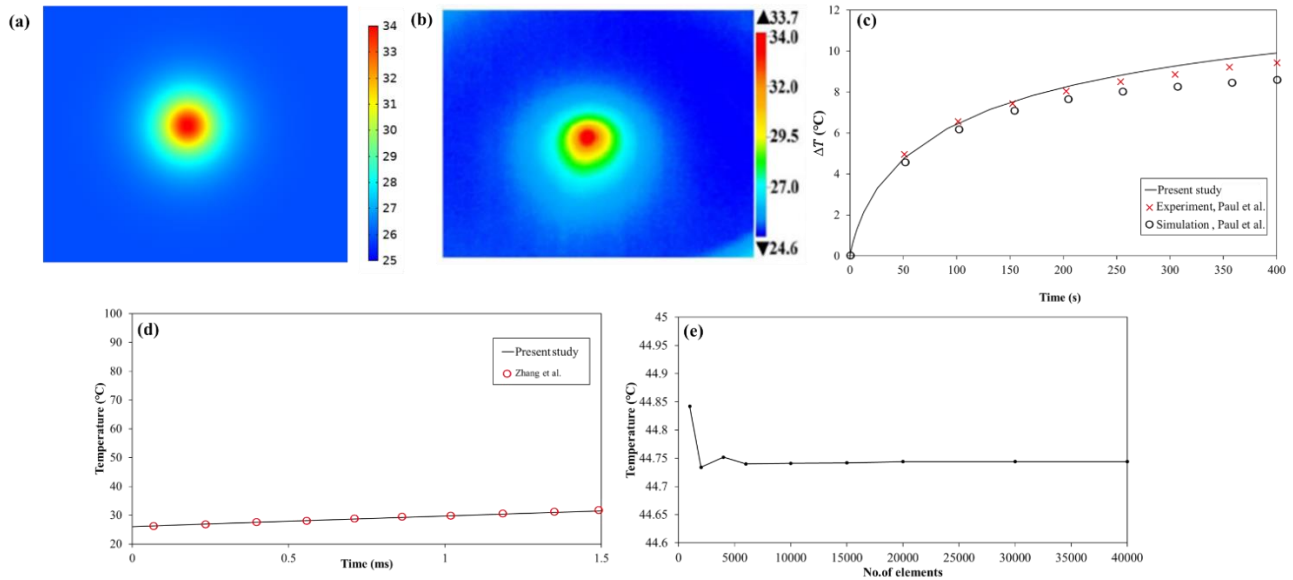
5  
6 The experiment and simulation results obtained by the previously published work of Paul et al. [23] were used to  
7 investigate the accuracy of this present numerical model under identical testing conditions. In Paul's simulation, laser  
8 absorption energy is described by Beer-Lambert's law. In Paul et al.'s experiment, a tissue phantom (agar) was irradiated  
9 with a continuous-wave laser of 800 nm. The diameter and height of the tissues was 10 cm and 15 cm, respectively. The  
10 intensity of the incident laser beam on the tissue phantom is 32000 W/m<sup>2</sup>, and the radius of the laser beam ( $\sigma$ ) is 2.5 mm.  
11 The ambient temperature is 25 °C and considering convective heat transfer of 10 W/(m<sup>2</sup>·K)). In this validation, The incident  
12 laser power is considered as a Gaussian distribution according to the following expression:

$$P_{laser} = P_0 \exp(-r^2/2\sigma^2) \quad (14)$$

13  
14  
15  
16 The intensity of the incident laser beam on the tissue phantom ( $P_0$ ) is 32000 W/m<sup>2</sup>, and the radius of the laser beam ( $\sigma$ ) is  
17 2.5 mm [23]. The optical and physical properties of phantom tissue are in Table 2.

18 In addition, the numerical results obtained by Zhang et al.[44], similar work is also validated under the same  
19 conditions. The light transport equation is used in Zhang's model to calculate the laser energy within skin tissue in birthmark

1 treatment by laser irradiation with fluence of  $8 \text{ J/cm}^2$  of 1.5 ms of time irradiation. From the validation results as shown in  
 2 Figure.2 (a-d) represents the surface temperature from (a) the present model, (b) Paul et al.'s experiment, (c) the comparison  
 3 of temperature change over time between the present numerical results, experimental results, and simulation results obtained  
 4 from Paul et al.[23], and (d) The validation results of the skin surface temperature, against Zhang et al.[44]. It shows a great  
 5 deal of consistency with the contour temperature and temperature data, which similar trend of temperature profile. Hence, it  
 6 provides credibility to the precision of the present numerical models.  
 7



8  
 9 Figure 2.(a) the present model results (top view), (b) Paul et al.'s experimental results [23], (c) validation results of present  
 10 study against experimental results obtained by Paul et al.[23], (d) validation results of present study against numerical results  
 11 obtained by Zhang et al.[44], and (e) model's grid convergence curve.

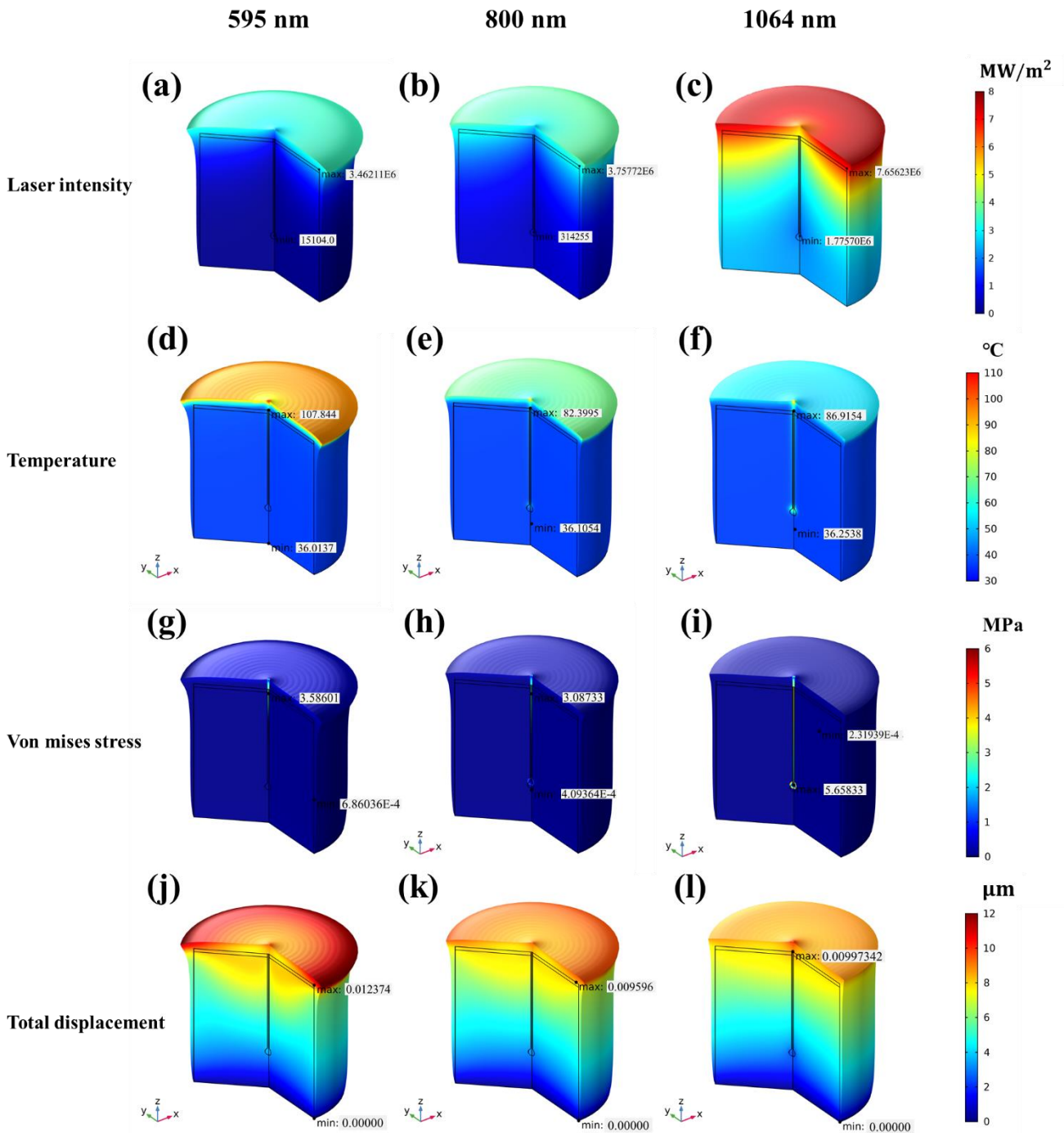
12  
 13 **5. Result and Discussion**

14  
 15 Naturally, when irradiating the skin with a laser, the two primary phenomena that occur in tissues are light absorption  
 16 and heat generation. The laser light is absorbed by the tissue and converted to heat energy. Due to the unequal absorption  
 17 coefficients and scattering, the amount of laser deposition in each tissue layer is different, directly resulting in treatment  
 18 outcomes. Nevertheless, since skin tissue is a bio-elastic material, the mechanical deformation of thermal expansion could  
 19 also occur. Consequently, the phenomenon of skin deformation during treatment must also be considered. During laser hair  
 20 removal treatments, high temperatures can lead to thermal damage from undesired heat and mechanical deformation in the  
 21 skin tissue arising in painful sensations. Controlling the heating and limiting the heated area is essential. Thus, comprehensive  
 22 treatment outcome prediction of phenomena that possibly occur before the actual treatment assists physicians in improving  
 23 safer and more effective therapeutic plans. In this section, the influence of wavelengths on temperature distribution and  
 24 deformation of skin tissue during the laser hair removal treatment is investigated and illustrated.

25  
 26 **5.1 Laser intensity distribution**

27  
 28 Figure.3 (a-c) shows a 3D simulation of the laser intensity distribution within skin tissue layers and hair after 50 ms  
 29 of laser irradiation with a laser fluence of  $5 \text{ J/cm}^2$  of 595 nm, 800 nm, and 1064 nm. At all wavelengths, the laser intensity  
 30 distribution can be clearly observed at the epidermis site. Even though the input of laser fluence is the same in all cases, the  
 31 simulation reveals that 1064 nm laser deposits the most energy within skin tissue, followed by 800 nm and 595 nm,  
 32 respectively. Figure.7 (a), which depicts the laser intensity lines of 595 nm, 800 nm, and 1064 nm on the surface skin (r-axis  
 33 and z=0 mm), provides confirmation. The 1064 nm laser intensity line is the most intense at the skin's surface (epidermis  
 34 layer). After skin tissue receives laser energy, all wavelengths decrease gradually along the longitudinal axis to the bottom  
 35 of the skin. Figure.7 (b) depicts the 595 nm, 800 nm, and 1064 nm laser intensity lines within hair tissue (z-axis and r=0 mm).  
 36 It indicates that 1064 nm laser energy can effectively reach the hair follicles. In contrast, the laser intensity lines of 595 nm  
 37 and 800 nm are marginally distinct and less intense than those of 1064 nm. In comparison, 595 nm and 800 nm treatment  
 38 performed poorly and was maintained at a low laser intensity level. Because the characteristics of the skin's light propagation  
 39 and ability to penetrate vary with wavelength. It can be mathematically explained using the optical diffusion coefficient

1 depicted in Figure 4. It displays the comparison of the optical diffusion coefficient of skin tissues at 595 nm, 800 nm, and  
 2 1064 nm. The epidermis, dermis, and hair optical diffusion coefficients are clearly different. The highest optical diffusion  
 3 coefficient in all tissues is 1064 nm, followed by 800 nm and 595 nm, respectively.  
 4



5  
 6  
 7 Figure.3 The 3D laser intensity (a-c), temperature (d-f), Von Mises stress (g-i) and displacement distribution (j-i) at wavelengths of 595  
 8 nm , 800 nm, and 1064 nm , laser fluence of 5 J/cm<sup>2</sup> at irradiation time 50 ms.  
 9



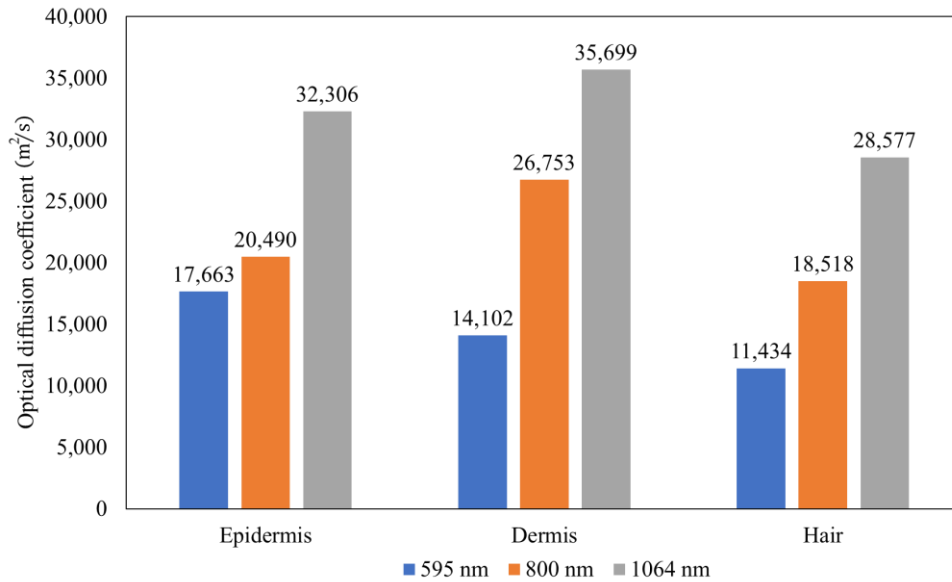


Figure.4 Comparison of the optical diffusion coefficient of skin tissues at 595 nm, 800 nm, 1064 nm.

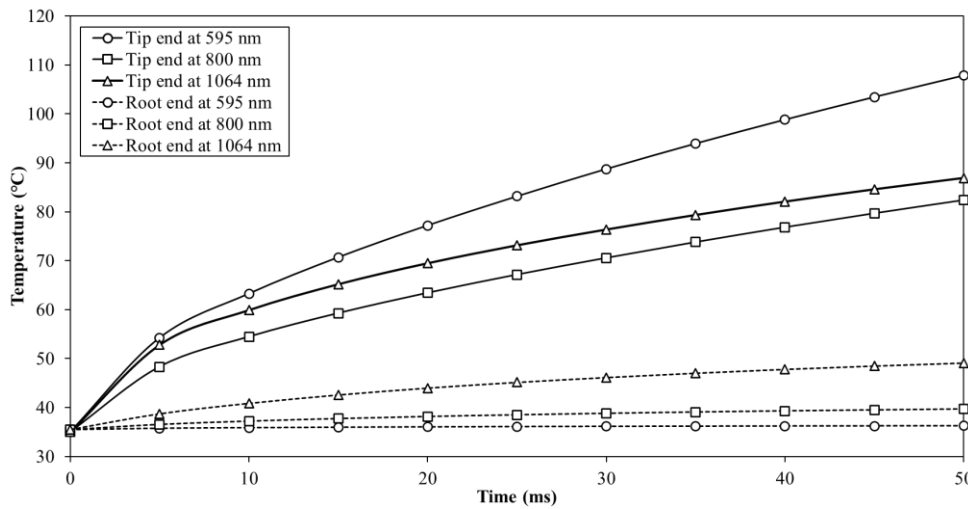
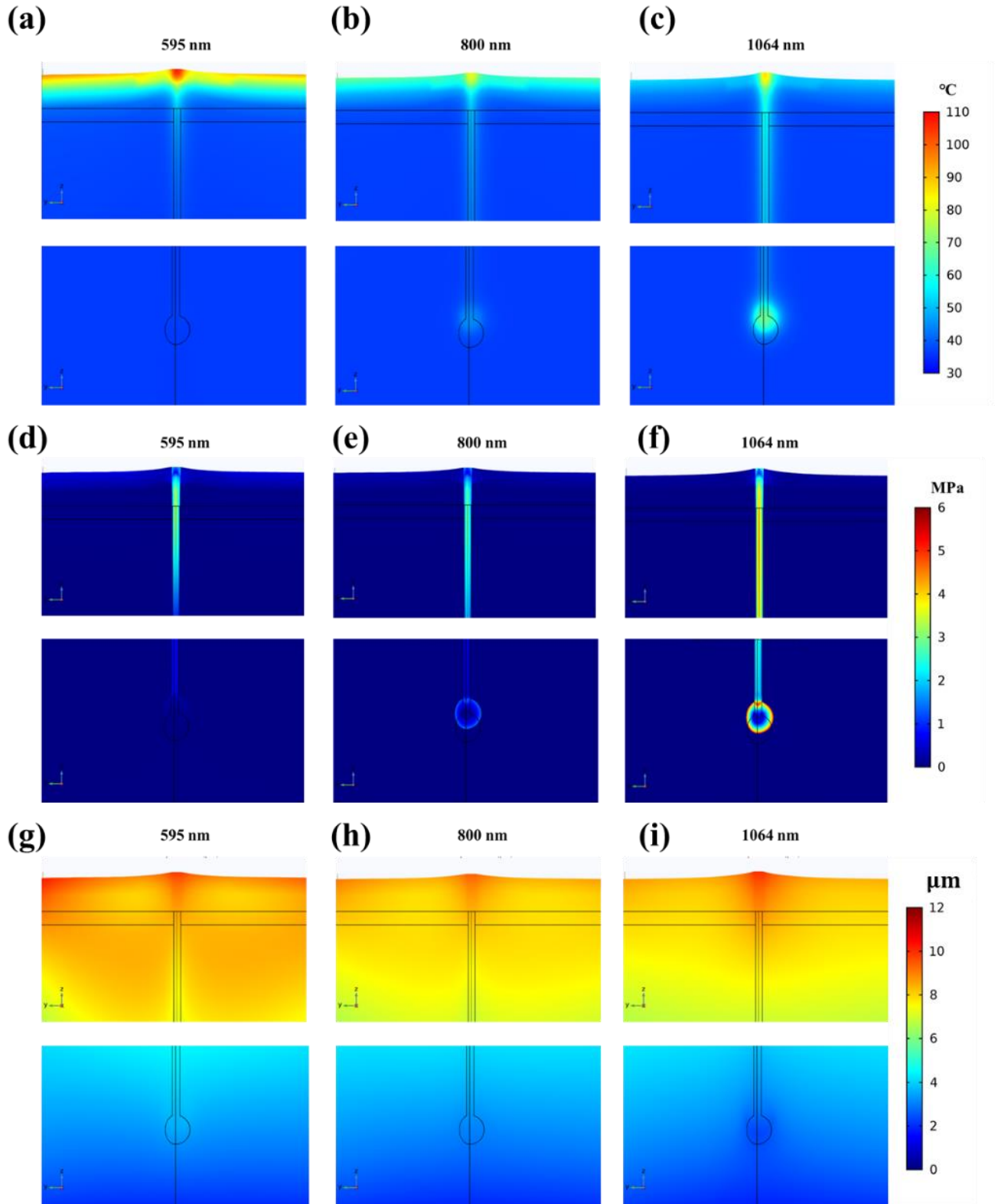


Figure.5 The temperature changes at laser irradiation 0-50 ms at hair tip and hair root after treatment with wavelengths of 595 nm, 800 nm, and 1064 nm.

## 5.2 Temperature distribution

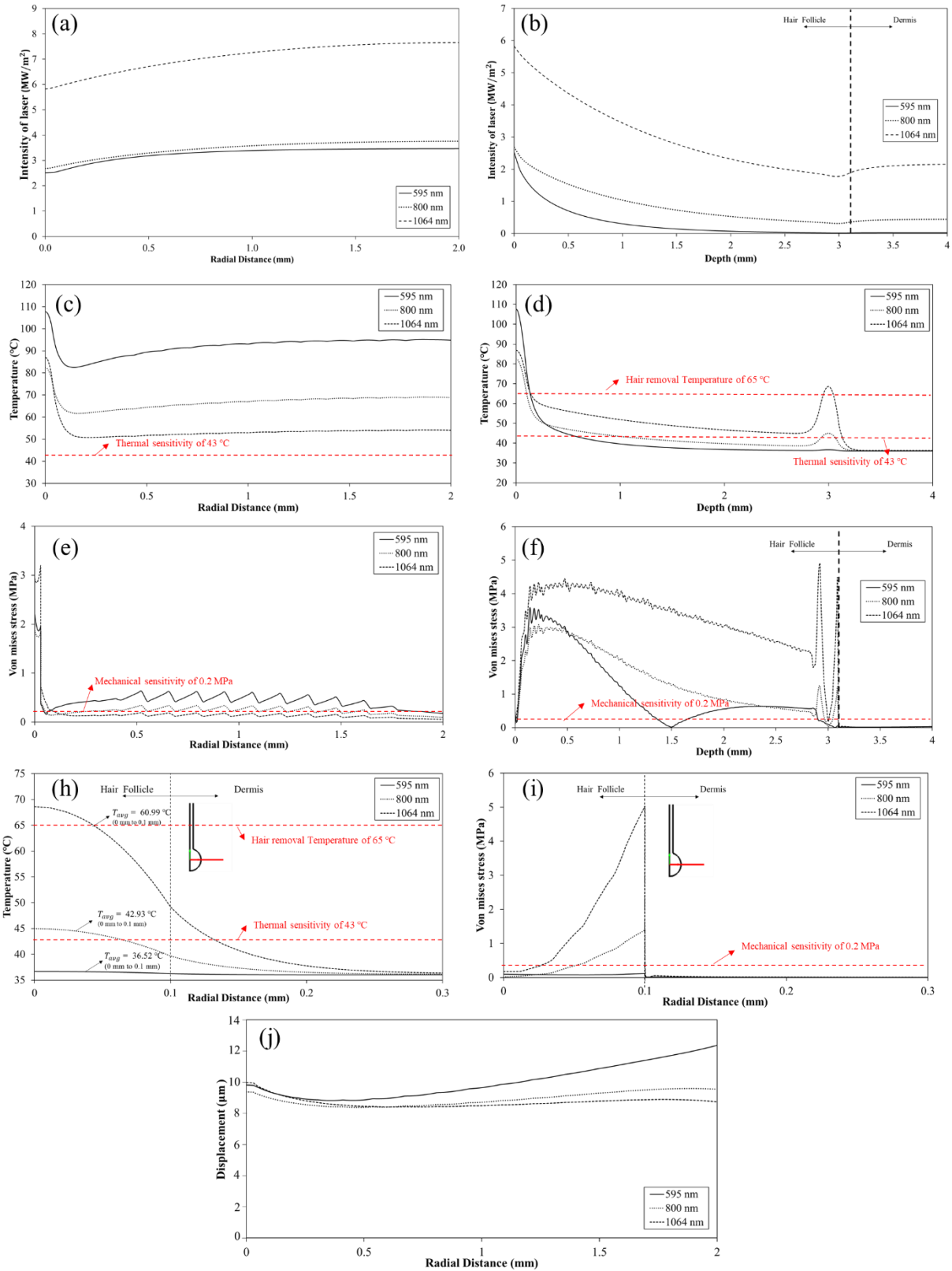
Figure.3 (a-c) shows a 3D simulation of the temperature profile in skin tissue layers and hair after 50 ms of laser irradiation with a laser fluence of 5 J/cm<sup>2</sup> at 595 nm, 800 nm, and 1064 nm. The amount of laser energy absorbed by skin varies according to wavelength. After absorbing laser energy, it is converted into thermal energy. As shown in Figure.3 (a-c), a large amount of absorbed energy in the epidermis leads to the high surface temperature of the skin. The highest temperature occurred in the laser projection region's center (the hair's tip). The maximum temperature values at laser irradiation at 50 ms at 595 nm, 800 nm, and 1064 nm are 107.8440 °C, 82.3995 °C, and 86.9154 °C, respectively. To see the contour clearly, we have enlarged the image as shown in Figure 5(a-c). Although the laser intensity of 595 nm and 800 nm in epidermis tissue is very close as shown in Figure.7 (a), it is clearly seen that the temperature that occurred is quite different. Including the case of 1064 nm, which has the most significant intensity of laser depositing in epidermis tissue, delivered the lowest temperature. The results show that a wavelength of 595 nm produced the highest surface temperature (epidermis), followed by 800 nm and 1064 nm, respectively. The absorption coefficients of skin tissues such as the epidermis, dermis, and hair vary with each wavelength. It can be clearly seen in the case of 595 nm that the laser deposition within epidermis tissue is the smallest but produces the highest temperature. The optical absorptivity of epidermal tissue at a wavelength of 595 nm is higher than 800 nm and 1064 nm, resulting in higher temperatures on the surface, as evidenced by the absorption coefficient in Table 1.



2  
3 Figure.6 The 2D model of temperature (a-c), Von Mises stress (d-f) and the displacement distribution (g-i) at wavelengths of 595 nm , 800  
4 nm and 1064 nm , laser fluence of  $5 \text{ J/cm}^2$  at irradiation time 50 ms.

5  
6 In Figure.3(d-f), although the laser irradiation of 595 nm induced the highest temperature on the skin surface, the  
7 increase in temperature within the hair and hair follicles was not as effective. It can be seen in Figure 3. (b-c) that the  
8 temperature of hair and hair follicles will be grander when exposed to longer wavelengths. Specifically, in the case of 1064  
9 nm, hair follicle temperature is greater than at other wavelengths. The optical diffusion coefficient impacts deep targeted  
10 tissue which in this case is hair follicles, receiving light energy and converting it to heat energy resulting in the maximum  
11 temperature occurring in hair follicles, even though the optical absorption coefficient is less than 595 and 800 nm. The hair

1 follicle's temperature dropped when the wavelength decreased by 800 nm and 595 nm, respectively, as related to Figure.5,  
 2 which presents the temperature changes at laser irradiation 0-50 ms at the hair tip and hair root after treatment with  
 3 wavelengths of 595 nm,800 nm, and 1064 nm. The temperature of hair tips is always significantly greater than hair roots.  
 4 After irradiation, the temperature of hair tips increases rapidly in all cases. In the case of 1064 nm, the temperature of root  
 5 hair rises gradually, whereas, in the case of 800 nm, it rises slightly. While temperature barely rises in the case of 595 nm.



6  
 7  
 8 Figure 7. (a-b) Laser intensity distribution along the radial direction and longitudinal direction (a-b) Temperature distribution  
 9 along the radial direction and longitudinal direction, (c-d) Von Mises stress distribution along the radial direction and  
 10 longitudinal direction, (e) comparison of the temperature of hair follicles, (f) comparison of Von Mises stresses of the hair

1 follicle, (g) Total displacement along the radial direction, and all are illustrated at laser fluence of  $5 \text{ J/cm}^2$  of 50 ms of  
2 irradiation time at wavelength of 595 nm, 800 nm, and 1064 nm.

3  
4 Figure.7(c) and Figure.7(d) depict the temperature distribution of skin tissue along the radial ( $r$ -axis and  $z=0 \text{ mm}$ ) and  
5 longitudinal ( $z$ -axis and  $r=0 \text{ mm}$ ) axes of different wavelengths at an irradiation time of 50 ms, respectively. Due to the higher  
6 absorption coefficient of hair, the center of laser irradiation (hair) is the highest temperature for all wavelengths. Nevertheless,  
7 it can be observed that the surface temperature of the skin tissue exceeds  $43 \text{ }^\circ\text{C}$  which is thermal sensitivity (the stimulus  
8 temperature of heat pain) in all cases, which may result in the undesired heating of the skin tissue, resulting in thermal injury  
9 later. In Figure.6(b), the potential of 1064 nm to produce heat at the center of the hair follicle ( $z = 3 \text{ mm}$ ) is greater than that  
10 of 595 nm and 800 nm, which is in good agreement with the previous discussions. Moreover, heating by laser irradiation  
11 does not have an effect on the temperature of tissue located beneath the hair follicle in the dermis. Figure.6 depicts the  
12 insertion of the temperature line within hair follicles ( $z = 3 \text{ mm}$  and  $0 \leq r \leq 0.3 \text{ mm}$ ) (e). The average temperature inside hair  
13 follicles ( $z = 3 \text{ mm}$  and  $0 \leq r \leq 0.1 \text{ mm}$ ) at 595 nm, 800 nm, and 1064 nm wavelengths. It is  $36.52 \text{ }^\circ\text{C}$ ,  $42.92 \text{ }^\circ\text{C}$ , and  $60.99$   
14  $^\circ\text{C}$ , respectively. Even though 1064 nm has the highest hair removal efficiency, the average temperature is still below the  
15 target temperature of  $65 \text{ }^\circ\text{C}$ . However, we observed that thermal damage could cause injury to the surrounding tissue (dermis),  
16 particularly at 1064 nm. It is due to the temperature difference between hair follicles and dermis tissue, which results in heat  
17 diffusion ( $r > 0.1$ ) nm. Consequently, using a higher fluence rate may also cause thermal damage to healthy tissue around  
18 hair follicles in the form of unwanted heat and it indicates that applying a laser of 1064 nm for therapy is better efficient than  
19 in the context of hair removal. The simulation results from the present model were consistent with previously explained  
20 research [15,18].

### 21 22 5.3 The Von Mises stress distribution.

23  
24 During laser hair removal, temperature gradients within the tissue caused a non-uniform thermal strain with skin  
25 tissue, resulting in a mechanical response such as stress within skin tissue. The stress occurred inside the skin tissue is  
26 considered as the one of essential parameter due to the skin can response to pain sensation from mechanical stress. Few works  
27 have been systematically discussed on this point in the past.

28 Figure.3(g-f) and Figure.6(d-f) present 3D models of Von Mises distribution in skin tissue layers and hair follicles  
29 after laser irradiation at 595 nm, 800 nm, and 1064 nm. From the simulation, the maximum stresses are 3.58601 MPa, 3.08733  
30 MPa, and 5.65833 MPa, respectively. In all cases, the highest values are observed in hair tissue. It is because influence of  
31 heat of laser energy to thermal strain of tissue. More significant temperature increases in hair increase thermal strain resulting  
32 in a high stress value within hair tissue. In addition, Young's modulus of hair is extremely high when compared to other  
33 tissues. However, we should concentrate on the epidermis and dermis, healthy tissues capable of responding to pain from  
34 mechanical sensations. As mentioned earlier, The lowest value of mechanical sensitivity leading to mechanical pain is 0.2  
35 MPa [7]. Figure.6(c) depicts the Von Mises stress distribution along the radial direction ( $r$ -axis and  $z=0 \text{ mm}$ ) after 50 ms of  
36 irradiation time. We observed that the stress also occurred on the surface, reaching the minimum value of mechanical  
37 sensitivity, especially in the case of 595 nm and 800 nm. We also observed that the trend of stress lines is agreeable to the  
38 temperature lines as shown in Figure.7 (c). It means that using 595 nm and 800 nm for treatment could result in mechanical  
39 pain sensations due to the stress value reaching the minimum of mechanical sensitivity 0.2 MPa (red line). In contrast, the  
40 stress is lower in a case of 1064 nm, which means that the patient will not experience mechanical pain during therapy. Instead,  
41 the patient may only feel pain due to thermal sensation. The temperature distribution is significantly related to the stress  
42 occurring within the skin tissue.

43 Figure.6(d) presents the Von Mises stress distribution along the longitudinal direction ( $z$ -axis and  $r=0 \text{ mm}$ ) after 50  
44 ms of irradiation time. It has been demonstrated that the stress arises in every instance along the length of the hair tissue. In  
45 the case of 1064 nm, the maximum stress at the hair tip decreases gradually along the longitudinal direction then it  
46 immediately rises at the hair follicles The same trend can be found in the case of 800 nm as well, but more slightly increased  
47 value, which is agree well to the laser intensity and temperature distribution as shown in Figure.7 (b),(d). While the case of  
48 595 nm is no stress in the hair follicles. In addition, we investigate the Von Mises stress distribution within hair follicles and  
49 the surrounding tissue by inserting lines at specific distances ( $z= 3 \text{ mm}$  and  $0 \leq r \leq 0.3 \text{ mm}$ ), as shown in Figure.7 (i). It  
50 indicates that there is no mechanical stress around the hair follicles. we also observed that the stress does not occur in the  
51 dermis tissue in all cases. It is no heat production, directing to a temperature that does not rise as well as mechanical stress.

52 The simulation results indicate that the severity of the physiological effects and mechanical deformation that small  
53 temperature increases will increase in sensitive organs such as skin tissue. For effective treatment, it is recommended to use  
54 a model that includes mechanical deformation to represent the actual behavior of tissue during laser hair removal and related  
55 therapy.

#### 5.4 The total displacement distribution.

The Von-Mises stress distribution is determined by the thermal expansion of skin tissue caused by the absorption of laser energy. Simultaneously, the displacement distribution of skin tissue also takes place. The effect of laser irradiation of wavelengths 595 nm, 800 nm, and 1064 nm is shown in Figure. 3 (j-l) and Figure.6 (g-i). It shows the total displacement distribution of skin tissue layers and hair after 50 ms of laser irradiation with a laser fluence of  $5 \text{ J/cm}^2$  at wavelengths of 595 nm, 800 nm, and 1064 nm. The simulation results revealed that the maximum displacement value occurred at the tissue's uppermost surface due to high temperature. Then, it decreases gradually in the direction of depth in all cases. In addition, we also present the total displacement along the radial direction ( $r$ -axis and  $z=0$ ) after 50 ms of laser irradiation at wavelengths of 595 nm, 800 nm, and 1064 nm, as shown in Figure.6 (g). Laser irradiation at 595 nm produced the most significant total displacement, followed by 800 nm and 1064 nm, respectively. The effect of temperature distribution induced by laser irradiation led to thermal expansion, which was observed clearly in the case of 595 nm, where the values of temperature and Von Mises stress are the highest at the skin's surface. During the therapy process, the temperature has a direct effect on the displacement of the skin. The laser's wavelength has a massive impact on the displacement of skin tissue. The shorter wavelength led to a greater displacement than the longer wavelength.

#### 6. Conclusion.

This study presents the photo-thermo-mechanical model coupling the light transport equation, bioheat transfer, and mechanical deformation in order to predict thermal and mechanical response. Systematically, the laser intensity, temperature, Von-Mises stress, and displacement were investigated. As shown in Figure.2 (a-d), the present model was in good agreement with the simulation and experimental results results obtained by Pual et al. [23], including the numerical results obtained by Zhang et al. [44]. Key findings that occurred from this study:

The wavelength of the laser has affected to the optical diffusion coefficient which results in the amount of laser deposition within skin tissue. The hair follicles better receive the laser energy when treated with 1064 nm, followed by 800 nm, and 595 nm, respectively.

The high-temperature area produces a high mechanical stress distribution with skin tissue during therapy as well as the displacement distribution.

In all wavelengths, the temperature at the skin's surface exceeds  $43 \text{ }^\circ\text{C}$ , meaning that the patient or client will experience thermal pain. However, treating with 595 nm and 800 nm may cause mechanical pain in patients, as the stress values are close to the mechanical sensitivity threshold of  $0.2 \text{ MPa}$  during laser hair removal.

This mathematical model predicts skin tissue's laser intensity, temperature and mechanical deformation during laser hair removal. The performance of laser hair removal was systematically investigated. It is observed that applying different laser wavelengths during laser hair removal results in a very localized increase in skin tissue temperature. It was discovered that using laser wavelengths 595 nm and 800 nm resulted in over-temperature in epidermis tissue and ineffective hair removal. In contrast, applying a laser of 1064 nm demonstrated the highest efficacy for hair removal. It is evident that the target tissue, the hair follicle, experienced a greater increase in temperature than other tissues. Additionally, the surface temperature of skin tissue is observed to be lower. However, the skin's surface temperature was also high enough to cause thermal injury and pain during laser hair removal in all cases. The obtained temperature profile in skin tissue is utilized as input data for mechanical analysis. It was discovered that when a laser with a different wavelength is applied, Von Mises stress is also so different. In addition, It was found the relationship between temperature and Von Mises stress. The rise in temperature within dermal tissues increases Von Mises stress levels during laser irradiation, particularly in hair. The greatest amount of Von Mises stress values occurred in hair. It is because hair has the highest value of Young's modulus. However, the Von Mises stress distribution along the surface area was greater than the skin's mechanical sensitivity value. Moreover, it was discovered that the skin's displacement was also affected by temperature. Increasing skin temperature had a direct effect on the total displacement. The magnitude of skin surface temperature is anticipated to influence the deformation of skin tissue and the pain.

According to the results, it should consider increasing a laser fluence level for better hair removal in a case of 1064 nm. Applying a 595 nm and 800 nm laser might be appropriate for other medical applications. In addition, it might consider unwanted heating prevention by employing cooling equipment such as Gel, Cooling air, Etc. for higher safety. Hence, suitable therapeutic planning is essential for highly effective treatment outcomes as well as safety standards.

1 Nevertheless, the current model has some limitations because using the light transport equation to analyze the  
2 accumulation of laser energy in tissues. The calculation parameters, such as the refractive index and anisotropy, are required,  
3 which differ from Beer-Lambert's law, including the thermal expansion coefficient of tissue affecting the simulation result.  
4 In addition, this model was created using 2D asymmetric. It may not be appropriate to add organs or tissues such as blood  
5 vessels or tumors, and one should be careful.

6 This research is a case study for modeling for treatment prediction of laser hair removal that considers mechanical  
7 deformation. A comprehensive investigation of physical phenomena that might occur within tissue during therapy is essential,  
8 such as in this study focused on predicting temperature and Von Mises stress distribution, which can be used as a guideline  
9 for treatment preparation. However, mechanical effects and other physical phenomena should be investigated more  
10 clearly, e.g., moisture loss effects (blood and water evaporation) on absorption coefficient, temperature, mechanical stress,  
11 and deformation shape changing after laser treatment, including considering dermal tissue as a porous media. Previously  
12 mentioned phenomena may directly affect final results, which is the cause of inaccurate pre-diagnosis.

13 In the medical field, electromagnetic waves, microwave, infrared, laser, and other similar technologies have been  
14 utilized to produce thermotherapy treatments for biological tissue such as liver, breast, cardiac, prostate, etc. The  
15 mathematical model of tissue necessitates extensive study. The proposed mathematical model is adaptable to thermotherapy  
16 application and development. The preceding section's simulation results help the field comprehend how to accurately assess  
17 tissue temperature and stress during thermotherapy in various treatment situations. This research will help evaluate the trend  
18 of laser irradiation on biological tissue and predict therapeutic response. Alternately, in the context of numerical modeling  
19 research, the proposed model can be helpful for modeling-interested researchers, who can adapt it for use in medical  
20 simulation or related medical applications.

## 21 22 **Acknowledgement**

23  
24 This research project is supported by National Research Council of Thailand (NRCT) : (Contact No.N41A640213),  
25 Research and Innovation, NXPO (Grant number B05F630092, B05F640205), National Research Council of Thailand (Grant  
26 No. N42A650197 ) and the Thailand Science Research and Innovation Fundamental Fund (Grant No. 66082)

## 27 28 **References**

- 29  
30 [1] Massey, R. A., Marrero, G., Goel-Bansal, M., Gmyrek, R., & Katz, B. E. (2001). Lasers in dermatology: a review. *Cutis*, 67(6),  
31 477–484.
- 32 [2] Gold M. H. (2007). Lasers and light sources for the removal of unwanted hair. *Clinics in dermatology*, 25(5), 443–453.  
33 <https://doi.org/10.1016/j.clindermatol.2007.05.017>
- 34 [3] Lavker, R. M., Miller, S., Wilson, C., Cotsarelis, G., Wei, Z. G., Yang, J. S., & Sun, T. T. (1993). Hair follicle stem cells: their  
35 location, role in hair cycle, and involvement in skin tumor formation. *The Journal of investigative dermatology*, 101(1 Suppl),  
36 16S–26S. <https://doi.org/10.1111/1523-1747.ep12362556>
- 37 [4] Gault, D. T., Grobbelaar, A. O., Grover, R., Liew, S. H., Philp, B., Clement, R. M., & Kiernan, M. N. (1999). The removal of  
38 unwanted hair using a ruby laser. *British journal of plastic surgery*, 52(3), 173–177. <https://doi.org/10.1054/bjps.1999.3083>
- 39 [5] Anderson, R. R., & Parrish, J. A. (1983). Selective photothermolysis: precise microsurgery by selective absorption of pulsed  
40 radiation. *Science (New York, N.Y.)*, 220(4596), 524–527. <https://doi.org/10.1126/science.6836297>
- 41 [6] Xu, F., Lu, T. (2011). Introduction of Skin Biothermomechanics. In: *Introduction to Skin Biothermomechanics and Thermal*  
42 *Pain*. Springer, Berlin, Heidelberg. [https://doi.org/10.1007/978-3-642-13202-5\\_8](https://doi.org/10.1007/978-3-642-13202-5_8)
- 43 [7] McCleskey, E. W., & Gold, M. S. (1999). Ion channels of nociception. *Annual review of physiology*, 61, 835–856.  
44 <https://doi.org/10.1146/annurev.physiol.61.1.835>
- 45 [8] Carroll, L., & Humphreys, T. R. (2006). Laser–tissue interactions. *Clinical Dermatology*, 24(1), 2–7  
46 <https://doi:10.1016/j.clindermatol.2005.10.019>
- 47 [9] Neukam F.W., Stelzle F. (2010). Laser Tumor Treatment in Oral and Maxillofacial Surgery. *Physics Procedia* 5 (2010) 91–100
- 48 [10] Goldberg, D. J., & Silapunt, S. (2001). Hair removal using a long-pulsed Nd:YAG Laser: comparison at fluences of 50, 80, and  
49 100 J/cm. *Dermatologic surgery : official publication for American Society for Dermatologic Surgery [et al.]*, 27(5), 434–436.  
50 <https://doi.org/10.1046/j.1524-4725.2001.00329.x>
- 51 [11] Paithankar, D. Y., Ross, E. V., Saleh, B. A., Blair, M. A., & Graham, B. S. (2002). Acne treatment with a 1,450 nm wavelength  
52 laser and cryogen spray cooling. *Lasers in surgery and medicine*, 31(2), 106–114. <https://doi.org/10.1002/lsm.10086>
- 53 [12] Fiskerstrand, E. J., Svaasand, L. O., & Nelson, J. S. (2003). Hair removal with long pulsed diode lasers: a comparison between  
54 two systems with different pulse structures. *Lasers in surgery and medicine*, 32(5), 399–404. <https://doi.org/10.1002/lsm.10175>
- 55 [13] Svaasand, L. O., & Nelson, J. S. (2004). On the physics of laser-induced selective photothermolysis of hair follicles: Influence  
56 of wavelength, pulse duration, and epidermal cooling. *Journal of biomedical optics*, 9(2), 353–361.  
57 <https://doi.org/10.1117/1.1646174>



- 1 [14] Babilas, P., Shafirstein, G., Baier, J., Schacht, V., Szeimies, R. M., Landthaler, M., Bäumler, W., & Abels, C. (2007).  
2 Photothermolysis of blood vessels using indocyanine green and pulsed diode laser irradiation in the dorsal skinfold chamber  
3 model. *Lasers in surgery and medicine*, 39(4), 341–352. <https://doi.org/10.1002/lsm.20483>
- 4 [15] Sun, F., Chaney, A., Anderson, R., & Aguilar, G. (2009). Thermal modeling and experimental validation of human hair and skin  
5 heated by broadband light. *Lasers in surgery and medicine*, 41(2), 161–169. <https://doi.org/10.1002/lsm.20743>
- 6 [16] Ataie-Fashtami, L., Shirkavand, A., Sarkar, S., Alinaghizadeh, M., Hejazi, M., Fateh, M., ... & Mohammadreza, H. (2011).  
7 Simulation of heat distribution and thermal damage patterns of diode hair-removal lasers: an applicable method for optimizing  
8 treatment parameters. *Photomedicine and laser surgery*, 29(7), 509-515.
- 9 [17] Shirkavand, A., Ataie-Fashtami, L., Sarkar, S., Alinaghizadeh, M. R., Fateh, M., Zand, N., & Djavid, G. E. (2012). Thermal  
10 damage patterns of diode hair-removal lasers according to various skin types and hair densities and colors: a simulation study.  
11 *Photomedicine and laser surgery*, 30(7), 374–380. <https://doi.org/10.1089/pho.2011.3152>
- 12 [18] Kim, T. H., Lee, G. W., & Youn, J. I. (2014). A comparison of temperature profile depending on skin types for laser hair removal  
13 therapy. *Lasers in medical science*, 29(6), 1829–1837. <https://doi.org/10.1007/s10103-014-1584-6>
- 14 [19] Mármol, G. V., & Villena, J. (2019). New 3D in silico model of hair and skin heating during laser hair removal. *Res. J. Pharm.*  
15 *Med. Sci*, 3, 15-24.
- 16 [20] Jaunich, M., Raje, S., Kim, K., Mitra, K., & Guo, Z. (2008). Bio-heat transfer analysis during short pulse laser irradiation of  
17 tissues. *International Journal of Heat and Mass Transfer*, 51(23-24), 5511-5521.
- 18 [21] A. Bhowmik, R. Repaka, S.C. Mishra, K. Mitra, Thermal assessment of ablation limit of subsurface tumor during focused  
19 ultrasound and laser heating, *J. Therm. Sci.Eng. Appl.* 8 (1) (2015).
- 20 [22] Lee, S. L., & Lu, Y. H. (2014). Modeling of bioheat equation for skin and a preliminary study on a noninvasive diagnostic method  
21 for skin burn wounds. *Burns : journal of the International Society for Burn Injuries*, 40(5), 930–939.  
22 <https://doi.org/10.1016/j.burns.2013.10.013>
- 23 [23] Paul, A., & Paul, A. (2019). Thermomechanical analysis of a triple layered skin structure in presence of nanoparticle embedding  
24 multi-level blood vessels. *International Journal of Heat and Mass Transfer*, 148, 119076.  
25 <https://doi.org/10.1016/j.ijheatmasstransfer>
- 26 [24] Dua, R., & Chakraborty, S. (2005). A novel modeling and simulation technique of photo--thermal interactions between lasers  
27 and living biological tissues undergoing multiple changes in phase. *Computers in biology and medicine*, 35(5), 447–462.  
28 <https://doi.org/10.1016/j.combiomed.2004.02.005>
- 29 [25] Wongchadukul P. and Rattanadecho, P. "Implementation of a 3D Thermomechanical Model to Simulate Selection Laser Heating  
30 (Effects of Wavelength, Laser Irradiation Intensity, and Irradiation Beam Area" *International Journal of Thermal Sciences*, Vol  
31 134, pp. 321-336, 2018
- 32 [26] Wongchadukul, P., Rattanadecho, P., & Wessapan, T. (2019). Simulation of temperature distribution in different human skin  
33 types exposed to laser irradiation with different wavelengths and laser irradiation intensities. *Songklanakarin Journal of Science*  
34 *& Technology*, 41(3).
- 35 [27] Wongchadukul, P., & Rattanadecho, P. (2021). Mathematical Modeling of Multilayered Skin with Embedded Tumor Through  
36 Combining Laser Ablation and Nanoparticles: Effects of Laser Beam Area, Wavelength, Intensity, Tumor Absorption Coefficient  
37 and Its Position. *Journal homepage: http://iieta.org/journals/ijht*, 39(1), 89-100. <https://doi.org/10.18280/ijht.390109>
- 38 [28] H.H. Pennes, Analysis of tissue and arterial blood temperatures in the resting human forearm (reprint of 1948 article), *J. Appl.*  
39 *Physiol.* 85 (1998) 5–34. <https://doi.org/10.1152/jappl.1948.1.2.93>
- 40 [29] Wessapan, T., Srisawatphisukul, S., & Rattanadecho, P. (2011). Numerical analysis of specific absorption rate and heat transfer  
41 in the human body exposed to leakage electromagnetic field at 915 MHz and 2450 MHz. *Journal of Heat Transfer*, 133(5).
- 42 [30] Wessapan, T., & Rattanadecho, P. (2012). Numerical analysis of specific absorption rate and heat transfer in human head  
43 subjected to mobile phone radiation: effects of user age and radiated power. *Journal of heat transfer*, 134(12).  
44 <https://doi.org/10.1115/1.4006595>
- 45 [31] Wessapan, T., & Rattanadecho, P. (2012). Specific absorption rate and temperature increase in human eye subjected to  
46 electromagnetic fields at 900 MHz.
- 47 [32] Laubach, H. J., Makin, I. R., Barthe, P. G., Slayton, M. H., & Manstein, D. (2008). Intense focused ultrasound: evaluation of a  
48 new treatment modality for precise microcoagulation within the skin. *Dermatologic surgery : official publication for American*  
49 *Society for Dermatologic Surgery [et al.]*, 34(5), 727–734. <https://doi.org/10.1111/j.1524-4725.2008.34196.x>
- 50 [33] Li, C. H., Li, S. A., Huang, Z. H., & Xu, W. B. (2010). Skin Thermal Effect by FE Simulation and Experiment of Laser  
51 Ultrasonics. In *Applied Mechanics and Materials* (Vols. 24–25, pp. 281–286). Trans Tech Publications, Ltd.  
52 <https://doi.org/10.4028/www.scientific.net/amm.24-25.281>
- 53 [34] Montienthong, P., and Rattanadecho, P. (2019). Focused Ultrasound Ablation for the Treatment of Patients With Localized  
54 Deformed Breast Cancer: Computer Simulation. *ASME. J. Heat Transfer*. October 2019; 141(10): 101101.  
55 <https://doi.org/10.1115/1.4044393>
- 56 [35] Bhargava, D., Rattanadecho, P., & Wessapan, T. (2020). The effect of metal objects on the SAR and temperature increase in the  
57 human head exposed to dipole antenna (numerical analysis). *Case Studies in Thermal Engineering*, 22, 100789.  
58 <https://doi.org/10.1016/j.csite.2020.100789>.
- 59 [36] Preechaphonkul, W., & Rattanadecho, P. (2021). The comparative of the performance for predicted thermal models during  
60 microwave ablation process using a slot antenna. *Case Studies in Thermal Engineering*, 25, 100908.  
61 <https://doi.org/10.1016/j.csite.2021.100908>.

- 1 [37] Fung, Y. C. (1990). *Motion, Flow, Stress and Growth*. Biomechanics. Springer–Verlag.
- 2 [38] Sherrington, C. (1906). *The integrative action of the nervous system* Scribner. New York.
- 3 [39] Jor, J. W., Nash, M. P., Nielsen, P. M., & Hunter, P. J. (2007, August). Modelling the mechanical properties of human skin:  
4 towards a 3D discrete fibre model. In 2007 29th Annual International Conference of the IEEE Engineering in Medicine and  
5 Biology Society (pp. 6640-6643). IEEE. <https://doi.org/10.1109/IEMBS.2007.4353882>
- 6 [40] Garaizar, O. R., Qiao, L., Anwer, N., & Mathieu, L. (2016). Integration of thermal effects into tolerancing using skin model  
7 shapes. *Procedia Cirp*, 43, 196-201. <https://doi.org/10.1016/j.procir.2016.02.079>
- 8 [41] Larrabee Jr, W. F. (1986). A finite element model of skin deformation. I. Biomechanics of skin and soft tissue: a review. *The*  
9 *Laryngoscope*, 96(4), 399-405. <https://doi.org/10.1288/00005537-198604000-00012>
- 10 [42] Keangin, P., Wessapan, T., & Rattanadecho, P. (2011). Analysis of heat transfer in deformed liver cancer modeling treated  
11 using a microwave coaxial antenna. *Applied Thermal Engineering*, 31(16), 3243-3254.  
12 <https://doi.org/10.1016/j.applthermaleng.2011.06.005>
- 13 [43] Shafirstein, G., Bäumlér, W., Lapidóth, M., Ferguson, S., North, P. E., & Waner, M. (2004). A new mathematical approach to  
14 the diffusion approximation theory for selective photothermolysis modeling and its implication in laser treatment of port-wine  
15 stains. *Lasers in Surgery and Medicine: The Official Journal of the American Society for Laser Medicine and Surgery*, 34(4),  
16 335-347. <https://doi.org/10.1002/lsm.20028>
- 17 [44] Zhang, R., Verkruysse, W., Aguilar, G., & Nelson, J. S. (2005). Comparison of diffusion approximation and Monte Carlo  
18 based finite element models for simulating thermal responses to laser irradiation in discrete vessels. *Physics in Medicine &*  
19 *Biology*, 50(17), 4075. <https://doi.org/10.1088/0031-9155/50/17/011>
- 20 [45] Cheung, L., Mitrea, D., Suhrland, C., & Zeng, H. (2009). Laser Hair Removal: Comparative Study of Light Wavelength and its  
21 Effect on Laser Hair Removal.
- 22 [46] Ross, E. V., Ladin, Z., Kreindel, M., & Dierickx, C. (1999). Theoretical considerations in laser hair removal. *Dermatologic*  
23 *clinics*, 17(2), 333-355. [https://doi.org/10.1016/S0733-8635\(05\)70091-7](https://doi.org/10.1016/S0733-8635(05)70091-7)
- 24 [47] Lepselter, J., & Elman, M. (2004). Biological and clinical aspects in laser hair removal. *Journal of Dermatological Treatment*,  
25 15(2), 72-83.
- 26 [48] Kampen, T. v. (n.d.). Optical Properties of Hair. Retrieved April 21, 2021,  
27 from <https://pure.tue.nl/ws/files/47042193/632280-1.pdf>
- 28 [49] Steiner, R., Russ, D., Falkenstein, W., & Kienle, A. (2001). Optimization of Laser Epilation by Simulation of the Thermal Laser  
29 Effect. *Laser Physics*, 11 (1), 146-153.
- 30 [50] Shapshay, S. M. (1987). *Endoscopic Laser Surgery Handbook (Science and Practice of Surgery Series, No 10)*. New York:  
31 Marcel Dekker Inc.
- 32 [51] Xu, F., Lu, T. J., & Seffen, K. A. (2008). Biothermomechanics of skin tissues. *Journal of the Mechanics and Physics of Solids*,  
33 56(5), 1852-1884. <https://doi.org/10.1016/j.jmps.2007.11.011>
- 34 [52] Aguilar, G., Díaz, S. H., Lavernia, E. J., & Nelson, J. S. (2002). Cryogen spray cooling efficiency: Improvement of port wine  
35 stain laser therapy through multiple-intermittent cryogen spurts and laser pulses. *Lasers in Surgery and Medicine: The Official*  
36 *Journal of the American Society for Laser Medicine and Surgery*, 31(1), 27-35. <https://doi.org/10.1002/lsm.10076>
- 37 [53] Xu, F., Wen, T., Seffen, K., & Lu, T. (2008). Modeling of skin thermal pain: A preliminary study. *Applied mathematics and*  
38 *computation*, 205(1), 37-46. <https://doi.org/10.1016/j.amc.2008.05.045>
- 39 [54] Delalleau, A., Josse, G., Lagarde, J. M., Zahouani, H., & Bergheau, J. M. (2006). Characterization of the mechanical properties  
40 of skin by inverse analysis combined with the indentation test. *Journal of biomechanics*, 39(9), 1603-1610.  
41 <https://doi.org/10.1016/j.jbiomech.2005.05.001>
- 42 [55] Hendriks, F. M., Brokken, D., Oomens, C. W. J., Bader, D. L., & Baaijens, F. P. T. (2006). The relative contributions of different  
43 skin layers to the mechanical behavior of human skin in vivo using suction experiments. *Medical engineering & physics*, 28(3),  
44 259-266. <https://doi.org/10.1016/j.medengphy.2005.07.001>
- 45 [56] Yu, Y., Yang, W., Wang, B., & Meyers, M. A. (2017). Structure and mechanical behavior of human hair. *Materials Science and*  
46 *Engineering: C*, 73, 152-163. <https://doi.org/10.1016/j.msec.2016.12.008>
- 47